Seafloor geomorphology of convergent margins: Implications for Cascadia seismic hazard

Brian G. McAdoo, Mark K. Capone, and Justin Minder

Department of Geology, Vassar College, Poughkeepsie, New York, USA

Received 8 August 2003; revised 18 August 2004; accepted 16 September 2004; published 29 December 2004.

[1] We compare the geomorphology of several convergent continental margins to constrain the seismic hazard of the Cascadia margin offshore Oregon, and present the possibility of a slow earthquake mechanism for a characteristic Cascadia event. The Cascadia seafloor has a very delicate bathymetry, with well-preserved landslides and noneroded slopes approaching 20°, unusual for a margin that produces $M\sim9$ earthquakes. Three-dimensional seismic and multibeam bathymetry data from the Nankai Trough suggest ubiquitous erosion over the entire margin with a smooth lower slope, devoid of large landslides, as would be expected on an accretionary margin that produces $M\sim8.5$ earthquakes. The accretionary Makran (Pakistan) and Kodiak (Alaska) margins have evidence of mass wasting and smooth lower slopes that lack large landslides. The nonaccreting Nicaraguan, Sanriku, and Aleutian margins have large, well-preserved landslides that add roughness elements to the slope, and have produced anomalously large tsunami, suggesting a slow source mechanism. Quantitative analysis of the lower slope roughness suggests the Cascadia has a characteristic geomorphology substantially different than the other sedimented convergent margins. The geomorphology, heat flow, pore pressure regime, and accounts of the 1700 ''megathrust'' event suggest a possible characteristic earthquake with a slow source mechanism. Rupture velocity would be high enough to be tsunamigenic, but accelerations would be low such that downslope erosion is minimal. To make the distinction between a slow and rapid source mechanism is critical in planning for seismic hazard in the Pacific Northwest. *INDEX TERMS:* 3022 Marine Geology and Geophysics: Marine sediments—processes and transport; 3045 Marine Geology and Geophysics: Seafloor morphology and bottom photography; 7230 Seismology: Seismicity and seismotectonics; 7223 Seismology: Seismic hazard assessment and prediction; 8105 Tectonophysics: Continental margins and sedimentary basins (1212); *KEYWORDS:* Cascadia, Nankai, tsunami, slow earthquakes, landslides, seafloor geomorphology. **Citation:** McAdoo, B. G., M. K. Capone, and J. Minder (2004), Seafloor geomorphology of convergent margins: Implications for Cascadia seismic hazard, *Tectonics*, *23*, TC6008, doi:10.1029/2003TC001570.

Copyright 2004 by the American Geophysical Union.
0278-7407/04/2003TC001570$12.00

1. Introduction

[2] Convergent margins are responsible for the most destructive of earth's tectonic processes. Subduction zone earthquakes and tsunamis are responsible for hundreds to thousands of deaths per year and millions of dollars worth of damage. To best assess the hazard associated with these regions, we must use all tools at our disposal. Seafloor geomorphology is rapidly becoming a very helpful additional tool as data coverage of the continental margins increases with time. This study seeks to use the geomorphology of the seafloor to help assess the seismic hazard potential for the Cascadia margin using data from several similar margins around the world.

[3] Large earthquakes and tsunamis have recurred on the Cascadia subduction zone in western North America every ~600 years [e.g., *Atwater et al.*, 1995]. The tsunamis have deposited sediment in marshes from northern California to Vancouver Island, and the most recent in 1700 A.D. was recorded in Japan [*Satake et al.*, 1996]. The geographic extent of the deposit locations suggests that the entire length of the subduction zone is locked. Heat flow and geodetic modeling suggests that the subduction zone must be locked from the continental shelf break to the base of the accretionary prism [*Hyndman and Wang*, 1993], and turbidites in various sea channels along the margin also suggest a margin-wide event [*Goldfinger et al.*, 2003]. An earthquake large enough to trigger a Pacific basin-wide tsunami should have left evidence in the seafloor geomorphology in addition to the sand layers in the salt marshes of the Pacific Northwest and turbidites in the offshore channels.

[4] *McAdoo et al.* [1997] noted steep, noneroded slopes at the base of the continental slope offshore Oregon, and *McAdoo et al.* [2000] noticed a regional paucity of landslides. As earthquakes are a major trigger of submarine landslides [*Hampton et al.*, 1996], there should be extensive geomorphic evidence of erosion on a margin that produces giant earthquakes.

[5] The Nankai accretionary margin, offshore southeastern Japan, is a good analog to the Cascadia subduction zone. Both Cascadia and Nankai have thick sediment cover that insulates a young, warm subducting plate (10 and 20 Ma, respectively), both have similar convergent rates (~4 cm/yr), and both have ''weak'' subduction faults as evidenced by the almost perpendicular alignment of the maximum principal stress and direction of crustal contraction as indicated from

geodetic data [*Wang*, 2000]. Yet Nankai has $M\sim8.5$ earthquakes every 100–300 years[*Ando*, 1975], where the evidence from Cascadia suggests a $M\sim9$ earthquake every $\sim$600 years [*Atwater et al.*, 1995].

[6] The continental slope is an excellent place to look for geomorphic evidence of past earthquakes. Unlike subaerial environments where overland flow of water is a dominant geomorphic agent, it does not rain underwater, and well-preserved submarine landslides play a large role in the evolution of submarine landscapes [*O'Leary*, 1993; *McAdoo et al.*, 2000]. Factors promoting submarine landslides include rapid accumulations of sediments, sloping seafloor, and high physical stresses such as wave loading and earthquakes [*Hampton et al.*, 1996]. During sea level lowstands, dissociation of gas hydrates can trigger landslides [*Kayen and Lee*, 1993], as can turbidity currents downcutting through steep-walled canyons [*McAdoo et al.*, 2000]. *Li and Clark* [1991] propose that slope instability is enhanced along subduction boundaries where faulting and large magnitude earthquakes associated with plate subduction may promote slope failure. On margins with as much in common geologically and tectonically as Nankai and Cascadia, one would expect to see similar morphologies that reflect the dominant geomorphic process earthquakes.

[7] On the portion of the Cascadia margin offshore Oregon, landslide frequency and style vary along strike with variations in the structural regime [*McAdoo et al.*, 2000]. *MacKay et al.* [1992] showed that in northern Oregon, the folds and faults of the accretionary prism tend to verge landward whereas in the south, structures verge seaward (which is the normal state on most convergent margins). Using visual observations from the *Alvin* submersible, multibeam bathymetry data and consolidation tests, *McAdoo et al.* [1997] found steep (18°), nonfailed seafloor in the region where landward verging structures dominate. Landslides are well defined but spatially infrequent in this region and have shorter and less steep headwalls and few have coherent masses at the base, suggesting weak material near the seafloor [*McAdoo et al.*, 2000]. In the region where seaward verging structures dominate, very large, numerous, and overlapping landslides maintain postfailure cohesion (as evidenced by rubble at the base) and have scars with steep and high headwalls, suggesting sediment overconsolidation [*McAdoo et al.*, 2000]. *Goldfinger et al.* [2000] document a series of Pleistocene ''superscale'' slumps that involve much of the southern continental margin, probably triggered by earthquakes. This morphology is suggestive of a landscape that has evolved with repeated large magnitude earthquakes.

[8] Landward vergence, which is less common on convergent margins than its seaward counterpart, is assisted by low basal décollement shear strength (caused by fluid overpressure in the due to rapid sediment deposition) and slope geometry [*MacKay et al.*, 1992; *MacKay*, 1995]. In Oregon, the regions of landward and seaward vergence are separated by a series of NW striking transform faults that cut through the incoming sediment section, the underlying oceanic crust, and the accretionary prism [*MacKay*, 1995]. *McCaffrey and Goldfinger* [1995] suggest that these strike-slip faults may partition the margin, providing zones of weakness that would prevent a rupture of the entire subduction zone in one event, but rather in a series of closely spaced (temporally) smaller magnitude earthquakes.

[9] This study uses the seafloor geomorphology of the Cascadia subduction zone (offshore Oregon) to assess seismic hazard by comparing it to margins with similar tectonomorphology and known earthquake histories (Figure 1). Using multibeam bathymetry, 3-D (Nankai) and 2-D (northern Oregon) seismic data from the continental slope, we compare the erosive style and mechanisms on the two margins. Using multibeam bathymetry data from the Kodiak (Alaska), Makran (Pakistan), Sanriku (N. Japan), and Nicaragua margins, we compare seafloor roughness to regional geology and historical seismicity to determine whether earthquake frequency and/or magnitude affect erosion. What is the dominant morphology on margins that exhibit a particular mode of seismicity (e.g., slow earthquakes)? If erosion leaves its mark on the seafloor, can a quantification of seafloor roughness aid in understanding how the seafloor responds to earthquakes? Can this roughness index be used to assess earthquake, offshore landslide and tsunami hazard on continental margins?

2. Tectonic Setting

2.1. Oregon

[10] The study area is located on the north central Oregon continental slope within the Cascadia accretionary prism. The accretionary prism along the northern California-Oregon-Washington margin is being created as the Miocene ($\sim$6 Ma) age Juan de Fuca plate is subducted beneath the North American plate at 42 mm/yr [*Kulm et al.*, 1986; *Demets et al.*, 1990]. The young crust with its thick, insulating sediment cover is particularly warm [*Hyndman and Wang*, 1993]. A bathymetric trench is not present due to large quantities of Pliocene/Pleistocene turbidite fill from the Columbia River by way of Astoria Canyon [*Cochrane et al.*, 1994]. Nearly all the sediment is accreted to the margin in northern Oregon (3.6 km of almost 4 km), compared to only two thirds of the sediment in the seaward vergent region [*MacKay et al.*, 1992]. Negative polarity seismic reflectors suggest fluid overpressuring on the basal décollement in the landward vergent region [*Moore et al.*, 1995]. In the region of the Astoria and Nitinat Fans, landward verging faults and folds suggest low coupling along the plate interface underneath the accretionary prism [*MacKay et al.*, 1992; *Fisher et al.*, 1999]. Large magnitude ($M\sim9$), tsunami-generating earthquakes occur every $\sim$600 years, as evidenced by both salt marsh tsunami deposits [*Atwater et al.*, 1995], and turbidites in the sea channels seaward of the slope base [*Goldfinger et al.*, 2003].

2.2. Nankai

[11] The Nankai margin has an accretionary prism formed as a $\sim$1.2 km thick sequence of hemipelagic sediment and turbidites overlying Miocene/Oligocene ($\sim$25 Ma) crust are

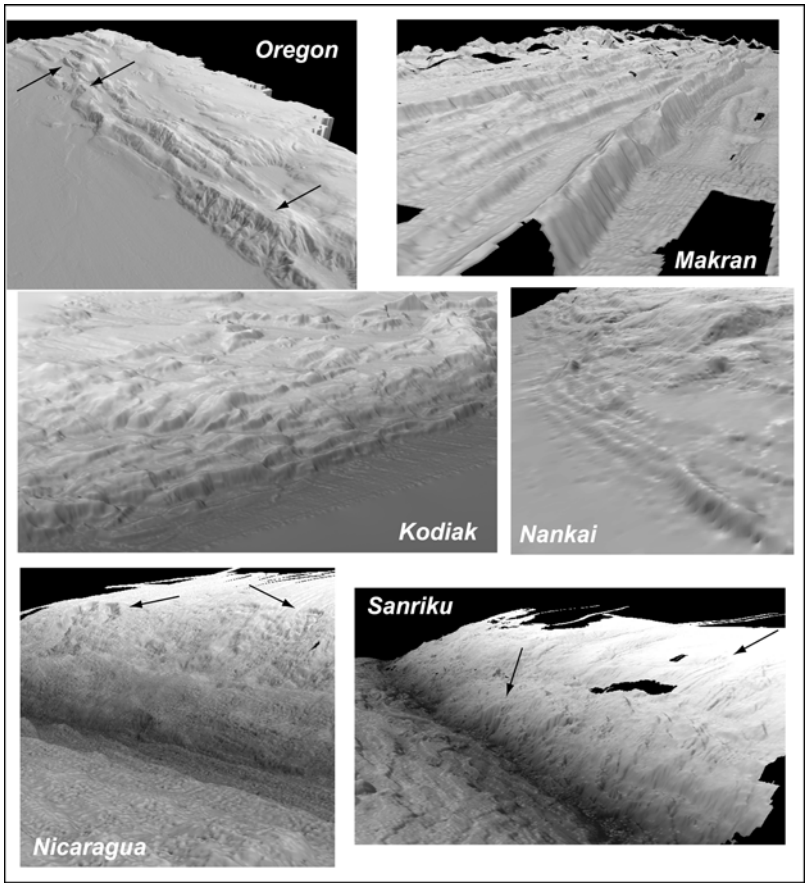

Figure 1. Three-dimensional perspective images of the margins offshore Oregon (Cascadia), Pakistan (Makran), Alaska (Kodiak), Shikoku (Nankai), Nicaragua, and Sanriku, showing similarities and differences in large-scale morphologies. Scale varies with perspective. Note the well-developed fold-and-thrust belts of the accretionary margins (Oregon, Makran, Kodiak, and Nankai), with the smooth limbs of the folds. Nicaragua and Sanriku do not have the sediment inputs as do the others, and therefore have a well-developed trench and a rougher lower slope. Arrows point to preserved landslide scars visible in the multibeam bathymetry data.

almost entirely scraped off the incoming Philippine Sea plate as it subducts underneath the Eurasian plate at a rate of 2–4 cm/yr, slightly oblique to the plate margin [*Karig*, 1986; *Seno et al.*, 1993]. The resulting accretionary prism has a well-developed fold-and-thrust belt similar to Cascadia. A deep embayment in the prism is and indentation caused as a series of seamounts impinges on the margin [*Yamazaki and Okamura*, 1989]. $M > 8$ earthquakes occur every 100–300 years, the most recent were the 1946 Nankaido (M_s = 8.2) and 1944 Tonankai (M_s = 8.0) earthquakes [*Ando*, 1975].

2.3. Other Margins

[12] We chose several other convergent margins with grossly similar tectonic and morphologic attributes for means of comparison. The Makran (Pakistan) and Kodiak (Alaska, NE Pacific) margins are both accretionary margins similar to Nankai and Cascadia with fold-and-thrust belts at the slope base. Nicaragua and Sanriku (N. Japan) are both margins that have produced tsunami earthquakes (events that produced large tsunamis relative to the surface wave magnitudes) and have significant landslide scars present on the continental slope.

[13] The Makran subduction zone results from the convergence of the Arabian plate with the Eurasian plate with an average convergent rate of 4 cm/yr, where convergence is nearly normal to the plate margin [*Byrne et al.*, 1992]. Abundant sediment supply (7 km thick) allows for a 350 km wide accretionary prism as the top 3–4 km are offscraped, with a well-developed fold-and-thrust belt that exhibits remarkably steep flanks [*Kopp et al.*, 2000; *Kukowski et al.*, 2001]. Slumping is identified on the upper slope above a midslope terrace from multibeam bathymetry data and 3.5 kHz subbottom data [*Kukowski et al.*, 2001; *von Rad and Doose*, 1998]. Erosion appears to be ubiquitous on the lower slope based primarily on qualitative assessments of seafloor morphology [*Kukowski et al.*, 2001]. Earthquakes recur every 100–200 years in $M \sim 8$ events [*Byrne et al.*, 1992].

[14] On the Kodiak margin, offshore southeast Alaska, the Pacific plate is being subducted underneath the North

American plate at a rate of around 5.5 cm/yr [*Demets et al.*, 1990], which is similar to Nankai and Cascadia. The crust is older (Eocene, 40–50 Ma) than the crust subducting in the Nankai trough and the crust being subducted at Cascadia, and has 1–2.5 km of overlying sediment [*Fruehn et al.*, 1999]. This is also the region of the 1964 M_s = 8.5 "Good Friday" earthquake.

[15] Over the distance of the Kodiak multibeam survey, the margin changes from accretionary in the southwest to erosional in the northeast [*Fruehn et al.*, 1999]. Accretion is locally disrupted by the subduction of seamounts, which causes an indentation of the deformation front and significant changes in slope morphology. The irregularities of the subducting basement are responsible for significant erosion of the lower slope [*Fruehn et al.*, 1999].

[16] In 1992, Nicaragua was hit by a M_s = 7.2 "tsunami earthquake" that had wave run-ups exceeding 10 m and killed over 100 people. A tsunami earthquake is an earthquake that produces a tsunami far larger than the surface wave magnitude would suggest, because of a very long source duration [*Kanamori and Kikuchi*, 1993]. Nicaragua is a nonaccreting margin: sediments are completely subducted, and the rupture from a given event may extend all the way to the seafloor. Rupture velocity is retarded by low velocity sediment that fill the plate boundary interface, therefore the short-period energy excited by rapid source mechanisms are not generated, and the longer period, tsunamigenic energy dominates [*Kanamori and Kikuchi*, 1993; *Satake*, 1994]. Submarine landslide scars are visible in the multibeam bathymetric data [*Ranero et al.*, 2000], as they are on the two margins with the most notable tsunami earthquakes recorded, 1946 Unimak Island (Aleutians) with a 35 m run-up from a M_s = 7.1 [*Fryer et al.*, 2004], and the 1896 Sanriku (Japan).

[17] In 1896, the Sanriku coast of northern Honshu, Japan was hit by a tsunami with up to 25 m of run-up following a relatively mild M_s = 7.2 earthquake [*Abe*, 1994; *Tanioka and Satake*, 1996]. The tsunami killed over 22,000 people 30 minutes after the mild shaking ended. *Cadet et al.* [1987] note large-scale slump features on the Sanriku continental slope. There is a small accretionary prism, and multichannel seismic data suggests that the incoming sediments are being subducted along the plate interface [*von Huene and Culotta*, 1989; *von Huene et al.*, 1994], as is the case in Nicaragua, slowing down the rupture velocity [*Tanioka and Satake*, 1996].

[18] Another margin of interest is the continental slope offshore Unimak Island in the northeastern Pacific. This is the epicentral region of the 1946 Aleutian Islands earthquake. This M_s = 7.1 earthquake produced a 35 m high tsunami that destroyed the Scotch Cap lighthouse on Unimak Island, and severe damage and deaths in Hilo, Hawaii. Run-up from this event extended to the Marquesas Islands (18 m run-up) and as far as the Antarctic Peninsula (4 m run-up [*Fryer and Watts*, 2001]). Neither seismic nor multibeam bathymetry is available in this region, but GLORIA side-scan sonar data [*Karl and Carlson*, 1996] suggest an exceptionally large (1625 km^2) and well-preserved submarine landslide, directly offshore from Scotch Cap [*Fryer et al.*, 2004](Figure 2).

3. Methods

[19] Multibeam bathymetry data are an excellent tool to use for a first pass geomorphic assessment of a continental margin. While it only provides a surface view of the seafloor, it is a relatively rapid and cost-effective tool when compared to seismic data acquisition and processing. Seismic data, if accessible, is used to assess the subsurface geology. Multibeam data are available for all margins in this study (Oregon, Nankai, Makran, Nicaragua, Kodiak, and Sanriku; Figure 1), and the 2-D and 3-D seismic data for Cascadia and Nankai respectively is not available over the entire multibeam survey area. The Oregon 2-D survey covers a region of seafloor around the transition from landward to seaward vergence [*MacKay et al.*, 1992]. Using the 2-D seismic data, we map regions of erosion where subseafloor reflectors are terminated at the seafloor reflection. Similarly, using the 3-D seismic data from Nankai, we use the seafloor reflector to get a detailed seafloor map (in depth and reflectivity), and map regions of erosion as where the subsurface reflectors terminate at the seafloor.

[20] The Oregon 2-D seismic survey consists of more than 2000 km of data [*MacKay et al.*, 1992]. The seismic source was a tuned 75 L air gun array fired at 25 m intervals, and reflections were received by a 144-channel streamer with group spacing of 25 m, yielding 72-fold common midpoint (CMP) data at a CMP interval of 12.5 m [*MacKay*, 1995]. The multibeam bathymetry from the National Oceanic and Atmospheric Administration is gridded at 100 m [*Grim*, 1992].

[21] The Nankai 3-D seismic survey is an 8 km by 80 km area beginning seaward of the deformation front and continues almost to the slope break. The survey was acquired using a source array of 14 air guns with a total volume of 70 L, fired at 50 m intervals [*Moore et al.*, 2001]. A 6 km long, 240-channel digital streamer with a group interval of 25 m received seismic reflection returns, yielding a 12.5 m CMP interval. The bathymetry data are from the Japanese Hydrologic Survey, gridded at 200 m.

[22] We used the multibeam bathymetry data for the first pass assessment of the dominant erosional morphologies on each of the margins. Visual evidence of erosion includes downslope gullies/rills, major canyons, landslides, and a general "rough" appearance. Three-dimensional visualization, artificial shading, slope gradient and aspect (cardinal direction of seafloor) maps highlight these features on the seafloor.

[23] To gain a quantitative assessment of seafloor roughness, we use the multibeam bathymetry data to calculate a surface area to planimetric area ratio (S/P; available at http://www.jennessent.com/arcview/surface_areas.htm). The S/P ratio is a good first pass at estimating the roughness as rugose slopes (i.e., rough) will have a higher S/P ratio than smooth slopes. However, smooth and steep slopes will also have a high S/P ratio. We chose an S/P ratio of 1.05, which reflects our visual assessment of "rough" seafloor. To

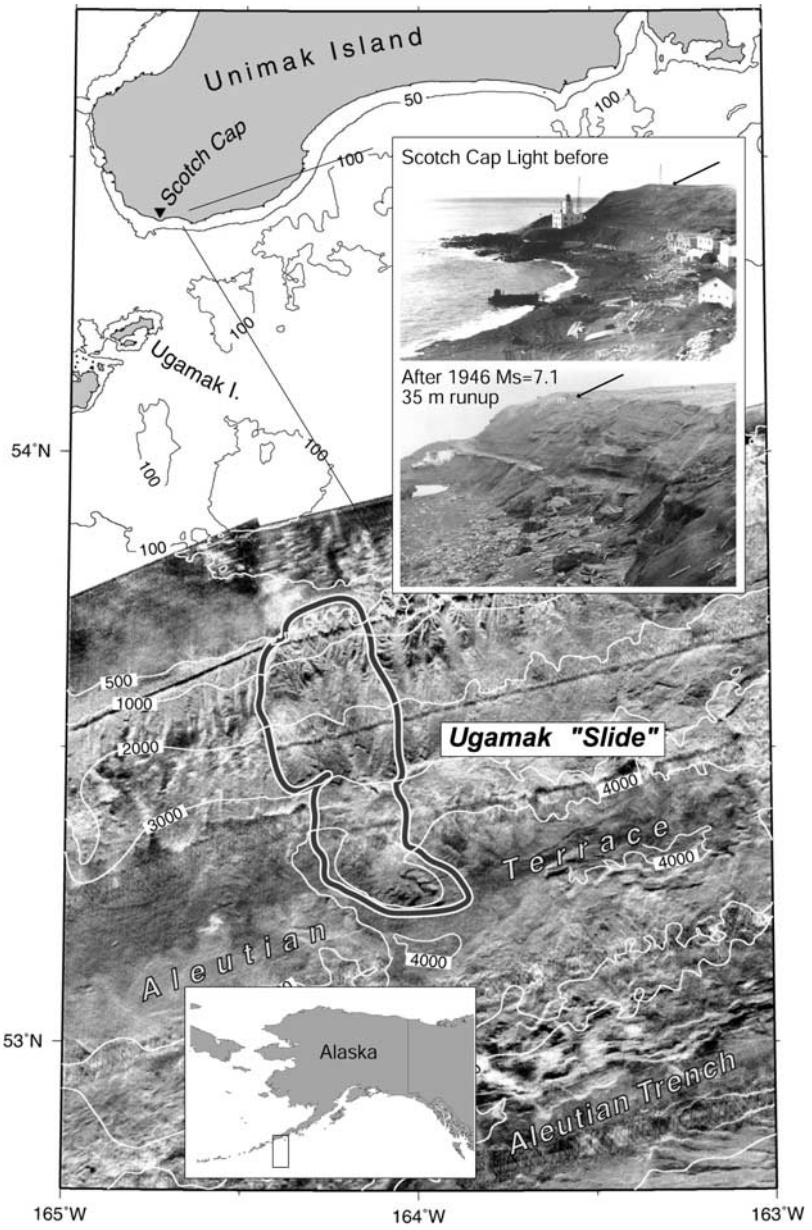

Figure 2. GLORIA data from the continental slope, offshore Unimak Island, Alaska. This is the epicentral region of the 1 April 1946, M_s = 7.1 earthquake, which produced a tsunami with more than 35 m run-up that destroyed the Scotch Cap Lighthouse (inset). Arrows point to the radio tower location (~35 m above sea level) before and after the tsunami. *Fryer et al.* [2004] suggest that the outlined feature is a possible large submarine landslide either triggered by the 1946 earthquake, or a preserved artifact from an earlier event (modified from *Fryer et al*. [2004], with permission from Elsevier).

distinguish between actual smooth slopes and smooth and steep slopes, we calculate the variance of both the slope gradient and the aspect. Seafloor with a diffusional profile will have a high slope gradient variance, but may not have a high aspect variance as those areas tend to slope in one direction (in the case of fold-and-thrust belts, normal to the strike of the structures). Aspect variance will be high in these fold-and-thrust belts as the flanks of the ridges face in opposite directions. To account for this, we only consider the downslope facing seafloor.

[24] After mapping regions of apparent erosion using the multibeam bathymetry data, we groundtruth our interpretations with the seismic data. Zones where subsurface reflectors terminate at the seafloor at high angles indicate erosion, and we create a seafloor horizon that highlights these zones. We then load the interpretations from the seismic data into a geographic information system (GIS), and compare zones of truncated reflectors with zones that have the appearance of erosion from the multibeam. Regions of truncated reflectors in the seismic data with the corresponding (“rough” versus

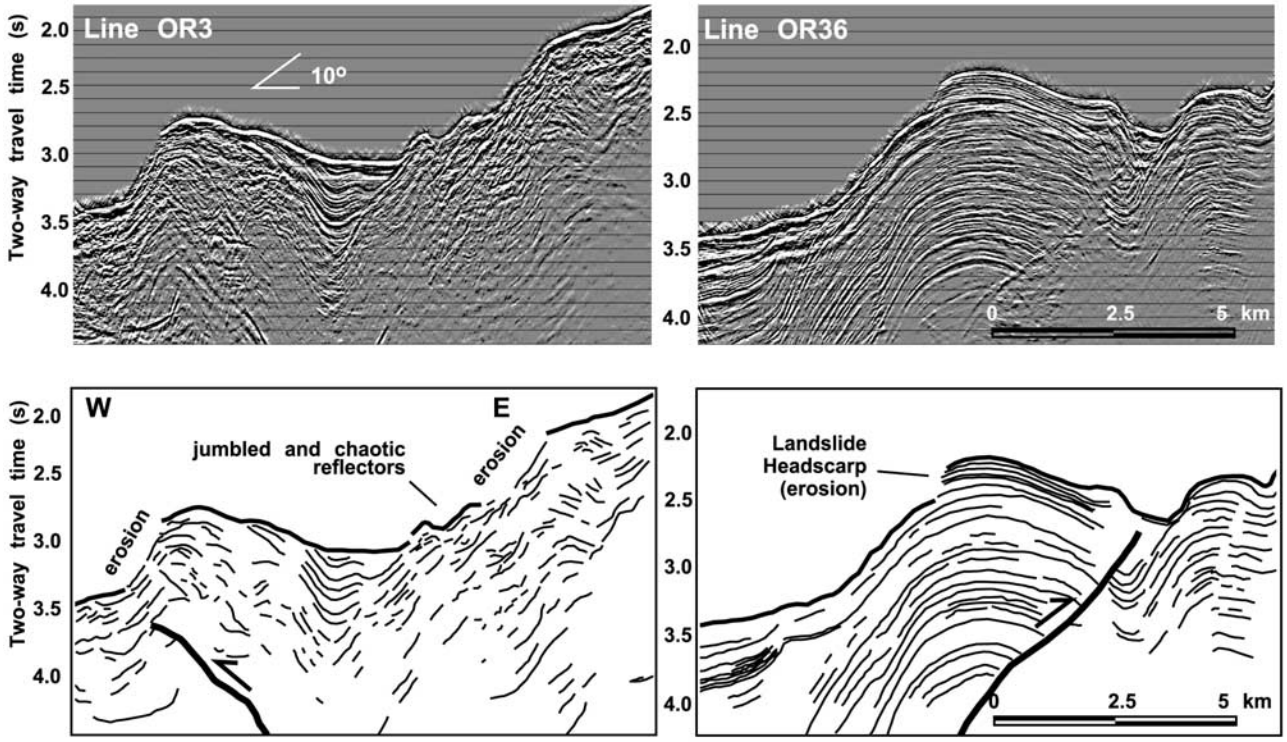

Figure 3. Two-dimensional seismic lines from the seaward and landward vergent regions of the accretionary prism offshore Oregon (see Figure 4 for location). Truncated reflectors indicate regions of erosion. The seaward vergent section (left) shows reflectors truncating at a high angle to the seafloor, suggesting a high degree of erosion, as do the discontinuous reflectors at the base of the slope. The example from the landward vergent region cuts through a landslide with a headscarp defined by truncated reflectors. Note the smooth, $\sim 10^{\circ}$ slope on the landward side of the landward verging anticline that is noneroded, and the continuous and nontruncated reflectors in the landslide scar, seaward of the headscarp.

"smooth") geomorphology then give us a regional signal of erosive morphology.

4. Observations

[25] Each of the margins in this study was chosen for morphologic similarities that tie them together. Cascadia is an accretionary margin with a substantial fold-and-thrust belt in the southern Washington/northern Oregon region that is dotted with large and well-defined landslides. Nankai, Makran, and, to a lesser extent, Kodiak, have a similar fold-and-thrust belts, but the flanks lack the well-defined landslides present in Cascadia. Nicaragua and Sanriku are not accretionary margins, but both have the large and well-defined landslides similar to those present in Cascadia, and each has a history of tsunami earthquakes. In this section, we will describe the nature of surface erosion in each area and quantifying these morphologies using the bathymetric data.

4.1. Cascadia

[26] In the seaward vergent region of south Oregon, the bathymetry data show regions of steep and rough seafloor. The overall character of the landward vergent region is smooth with patches of rough seafloor. Thirty-two of the seismic lines that run near perpendicular to the margin were interpreted for this study. Half of the lines were from the seaward vergent region south of 44.85°N and half were from the landward vergent region. On the basis of surface appearance and lateral extrapolation of the seismic data, the degree of seafloor erosion in the seaward vergent region is twice that of the landward vergent region.

[27] Examples of truncated seafloor and subseafloor reflectors in the seaward and landward vergent regions are shown in Figure 3 from the base of the accretionary prism. Line OR3 from the seaward vergent region shows the subseafloor reflectors terminate at high angles to the seafloor on the steepest slopes. On the downslope side of the terminations, the reflectors tend to be jumbled and chaotic. This is characteristic of the seismic data in the seaward vergent region. The seismic character of the landward vergent region differs substantially from the seaward vergent region. The seafloor reflector of Line 36 from the landward vergent region is truncated 2.6 km from the toe of the prism at the headscarp of a landslide with a mean slope of 28° [*McAdoo et al.*, 2000], but the failure surface has smooth and continuous seafloor and internal reflectors on an

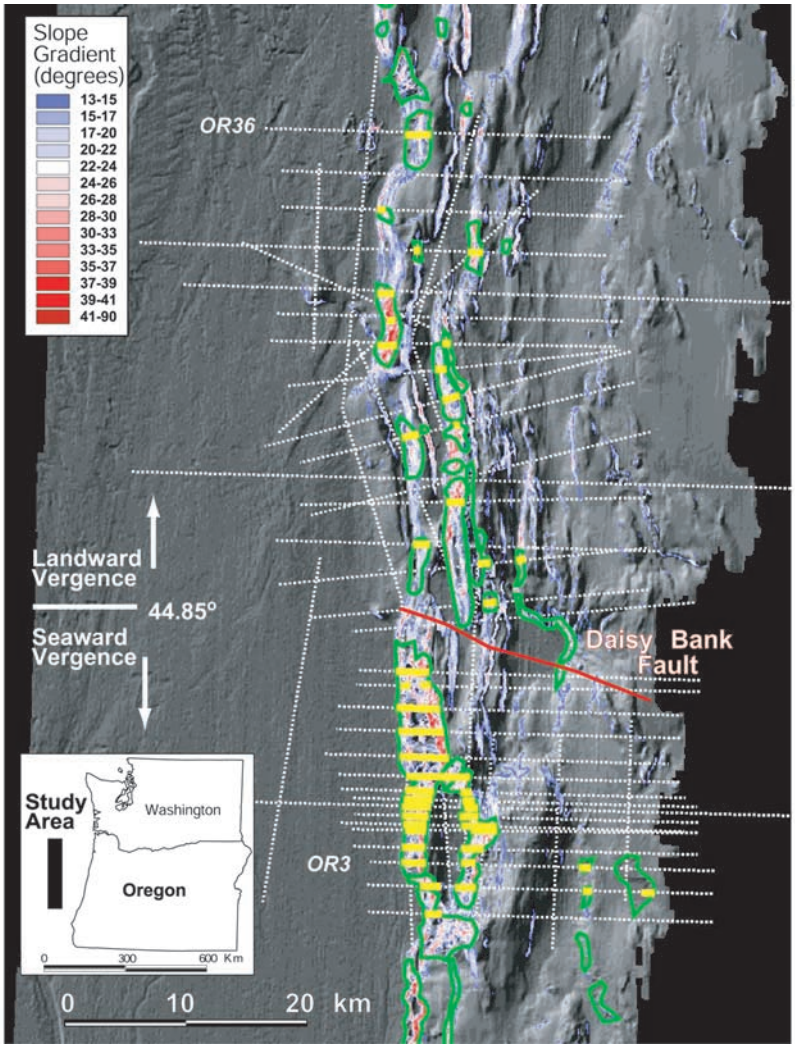

Figure 4. Shaded bathymetry and slope gradient of the Oregon continental slope in the region of the 2-D seismic survey (white lines). Yellow lines indicate regions on the underlying seismic lines with truncated reflectors (erosion), and areas outlined in green represent regions that appear to be eroded based on visual assessment of the multibeam bathymetry alone. Slope gradients less than 13° are transparent so that colors representing slope gradient occur only on slopes greater than 13°. Note regions where slopes exceed 13° and there is no bathymetric evidence of erosion and no truncated reflectors in the seismic data.

18° slope, and the landward facing side of the anticline has continuous reflectors on a ~10° slope.

[28] Using the bathymetry and seismic data in the GIS, we compared the seafloor morphology with the zones of truncated reflectors (Figure 4). Zones of anomalous seafloor roughness (visual assessment only) and previously mapped regions of mass wasting are highlighted [*McAdoo et al.*, 2000](Figure 1). Eight percent (124 of 1553 km^2) of the continental slope in the landward vergent region has considerably rough appearing seafloor compared to 19% (201 of 1060 km^2) of the seaward vergent region. The location of terminated reflectors, both seafloor and internal with the calculated the slope gradients for the region, are shown in Figure 3. Both regions have approximately the same spatial extent of slopes with gradients exceeding 30° (~35%), however the overall regional taper is significantly higher in the south (~4.3°) than in the north (~2.0°). Each of the internal reflectors in the seismic data that terminate at the seafloor occur on slopes greater than 15°. It is important to note that there are slopes present, mostly in the landward vergent region, with gradients greater than 15° with no evidence of reflector truncation or anomalous seafloor roughness (Figure 4).

[29] In summary, all truncated subseafloor reflectors coincide with the visually rough regions of areas on or near slopes approaching 15°, but there are slopes in the landward vergent area only greater than 15° without truncated reflec-

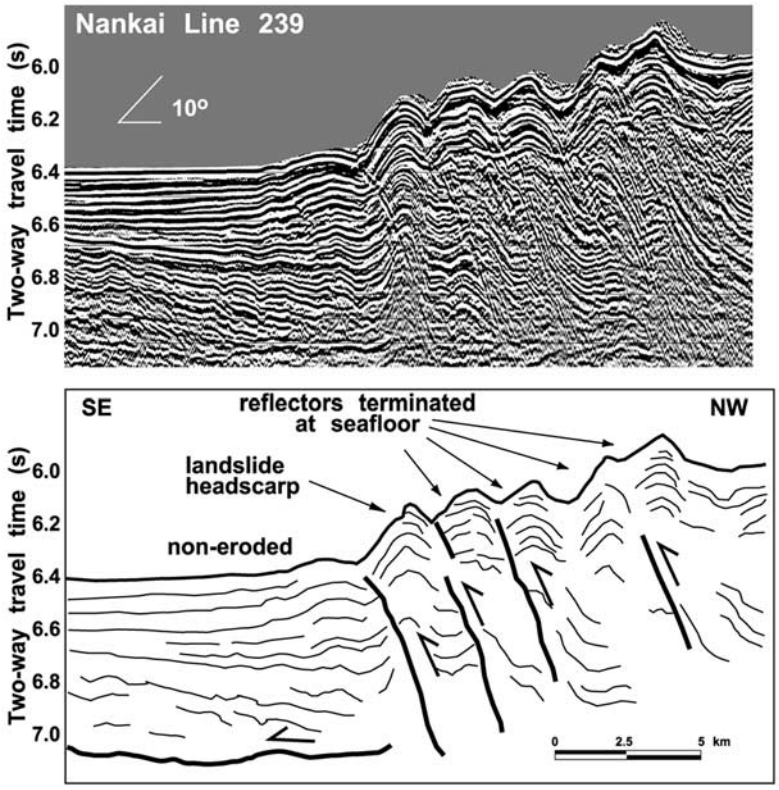

Figure 5. Line 239 from the Nankai 3-D seismic survey. Truncated reflectors occur on all slopes greater than 8° as evidenced by truncated reflectors in the seismic data, despite occurring on smooth seafloor. This section cuts through a landslide, and the headscarp is visible in the first substantial ridge. A nascent ridge in the basin has a slope of 3°, and is noneroded as reflectors are continuous to the basin. The faults and folds in this region are all seaward vergent.

tors. The majority of the truncated subseafloor reflectors correspond to areas of rough seafloor on slopes greater than 15°. A small proportion of bathymetrically rough areas do not show reflector truncation in the seismic data.

4.2. Nankai

[30] The multibeam bathymetry from Nankai has some characteristics that a very similar to the Oregon margin (Figure 1). The fold-and-thrust belt expresses itself as smooth anticline-syncline pairs. However the 3-D seismic data shows that the structures are seaward vergent and that erosion is extensive. All slopes exceeding 8° are eroded and midslope basins are the only regions upslope from the deformation front that are not eroded.

[31] We use the seafloor return from the 3-D seismic data to get a 50 m gridded bathymetry map. Figure 5 shows inline 239 at the base of the slope. The line cuts through a landslide, and the headscarp is shown clearly as a reflector terminated at a high angle with the seafloor. The eroded scar of the landslide is a 9° slope, and the average slope gradient outside the failure region is ~8°. The slope of the nascent ridge seaward of the slide is less than 3°, and has continuous reflectors along its length within the 3-D seismic survey area. Upslope from the second ridge with the landslide, the slope gradient varies between zero (on the ridgetops and basins) and a maximum of about 45°, 20 km landward of the slope base. The steepest slopes average approximately 20°, and the average gradient of the fold-and-thrust belt of the lower slope is 4.5°.

[32] Figure 6 shows extent of erosion in the Nankai 3-D seismic survey. All slopes greater than 8° have truncated reflectors as evidence of erosion. In marked contrast to the Oregon survey area, 64% of the Nankai survey area has terminated reflectors. If the region seaward of the deformation front is discounted, 80% of the margin exhibits some degree of erosion. The lowermost slope (first and second ridges) have gradients on noneroded slopes approaching 8°, but landward of the second ridge, every slope greater than 5° is eroded.

4.3. Seafloor Roughness

[33] Both Cascadia and Nankai have slopes with a smooth appearance; however, the seismic data suggest that one is substantially eroded (Nankai) while the other is in large part noneroded in the regions between large erosive features such as canyons and landslides. To distinguish

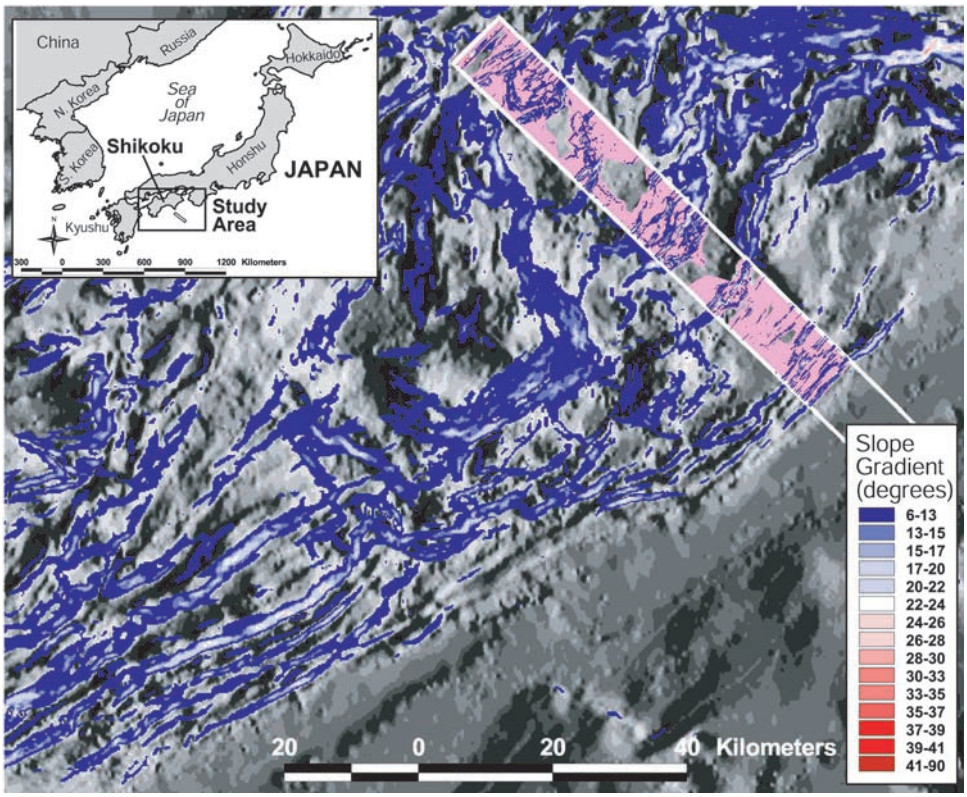

Figure 6. Shaded bathymetry and slope gradient of the Nankai continental slope in the region of the 3-D seismic survey (white box). Purple shading indicates regions on the underlying seismic data with truncated reflectors (erosion). Slope gradients less than 6° are transparent so that colors representing slope gradient occur only on slopes greater than 6°. The only noneroded regions in the 3-D survey upslope from the toe occur in slope basins that are actively receiving sediment from upslope.

between margins with a high degree of regional erosion and margins where erosion appears to be limited to large features, we used the multibeam bathymetry data to quantify seafloor roughness. Using Nankai and Cascadia as two end-members we compare erosive morphologies on the other margins by way of their roughness.

[34] We looked at roughness on two scales, one a continental margin-wide scale, and the other a 450 km^2 region at the base of the slope. The seafloor roughness at the slope base as evidenced by the slope gradient and aspect variance on slopes with a high surface to planimetric area ratio (S/P) is shown in Figure 7. The landward vergent section of Oregon margin, with its long ridges and occasional large landslides, has a very high slope variance with a low aspect variance. In the 450 km^2 region at the slope base, the aspect variance is higher due to the presence of landslides' sidewalls. The Kodiak and Nankai margins have high aspect variances, and moderate slope variances on a margin deformed by seamount collisions (Figure 8). The Makran has the lowest slope and aspect variances, which is possibly related to the very thick incoming sedimentary package providing a more homogeneous medium to deform. Nicaragua has high aspect variance with low slope variance, which may reflect a uniform slope with the only roughness elements due to the landslides. The data are summarized in the graphs in Figure 9.

5. Discussion

[35] The Nankai, Makran, and Kodiak accretionary margins have produced historic $M_s > 8$ earthquakes and tend to have smooth, highly eroded lower slopes with little evidence of large, well-preserved submarine landslides. Of the other margins in this study, Sanriku, Nicaragua, and the Aleutians have produced both large M_s earthquakes and so-called tsunami earthquakes (1898 Sanriku, 1946 Aleutians, 1992 Nicaragua) where very large tsunamis were produced considering the degree of shaking (i.e., M_s- surface wave magnitude) and each has noticeable offshore landslides. We propose that the degree of smoothness on a sedimented margin reflects the frequency of downslope erosive events that plane off roughness elements on the seafloor. Margins that have significant roughness elements, such as preserved scars of very large landslides, lack frequent downslope erosive flows, either because the margin is armored against small-scale slope failures (by lack of weak sediment), or the margins do not shake hard enough during the $M_s \sim 7$ earthquakes to diffuse the seafloor bathymetry, or some combination of the two. Because of these observations, we

suggest that Cascadia margin offshore Oregon, with its ample sediment supply, well-preserved landslides, and evidence for a substantial margin-wide earthquake and tsunami, produces slow earthquakes that do not shake the seafloor hard enough to trigger significant downslope erosive flows.

[36] Zones of subseafloor reflector truncation indicate regions of eroded seafloor. Using the bathymetry and seismic data of Nankai and Oregon, we extrapolate the zones of erosion from the seismic lines that correspond to the regions in the bathymetry data that appear to be eroded, then estimate the degree of overall erosion in the survey area (Figures 4 and 6). On the northern Oregon lower continental slope, erosion is limited on slopes less than 15°, compared to 8° on the Nankai margin, and in northern Oregon there are noneroded slopes greater than 15° whereas all slopes above 8° on Nankai are eroded. Areas with largely noneroded slopes exceeding 15° in Oregon's landward vergent region occur between discrete landslides, which are the most obvious erosional mechanism. In the seaward vergent region, erosion by way of numerous overlapping and discrete landslides is widespread [*McAdoo et al.*, 2000], yet scars are preserved suggesting large and perhaps temporally infrequent events.

[37] The large-scale morphology of the Nankai trough is similar to Oregon with its smooth flanked, fold-and-thrust belts, but the degree of erosion is far more extensive. The anticlinal ridges are very smooth because frequent erosive events consisting of nonconsolidated material have diffused the bathymetry. Downslope sediment transport is most likely accommodated by strong shaking that accompanies the $M \sim 8.5$ events that occur every 100–300 years [*Ando*, 1975]. Over time, the hundreds of earthquakes that occur between significant slope sedimentation events have the effect of eliminating small-scale roughness elements such as landslide headscarps, rubble, etc. that may or may not have ever been present. The resultant morphology is a smooth bathymetry with erosion on almost all slopes greater than 5°, and significant sediment ponding in the midslope basins. This is markedly different from the landward vergent region of Oregon where the smooth slopes between landslides indicates nonerosion.

[38] The other margins in this study that appear to have a similar erosive regime to Nankai are the Makran and Kodiak margins. The flanks of the anticlinal ridges at the slope base lack landslide scars and downslope erosion keeps the slopes free of rough elements. *Kukowski et al.* [2001] mention "small-scale" landsliding on the upper Makran slope, gullies and rills on the very steep (>20°) lower slope, and rapid sedimentation in midslope basins as evidence of downslope erosive flow, but these rills are too small to contribute significantly to the quantified roughness. *Fruehn et al.* [1999] discuss "considerable mass wasting" on the

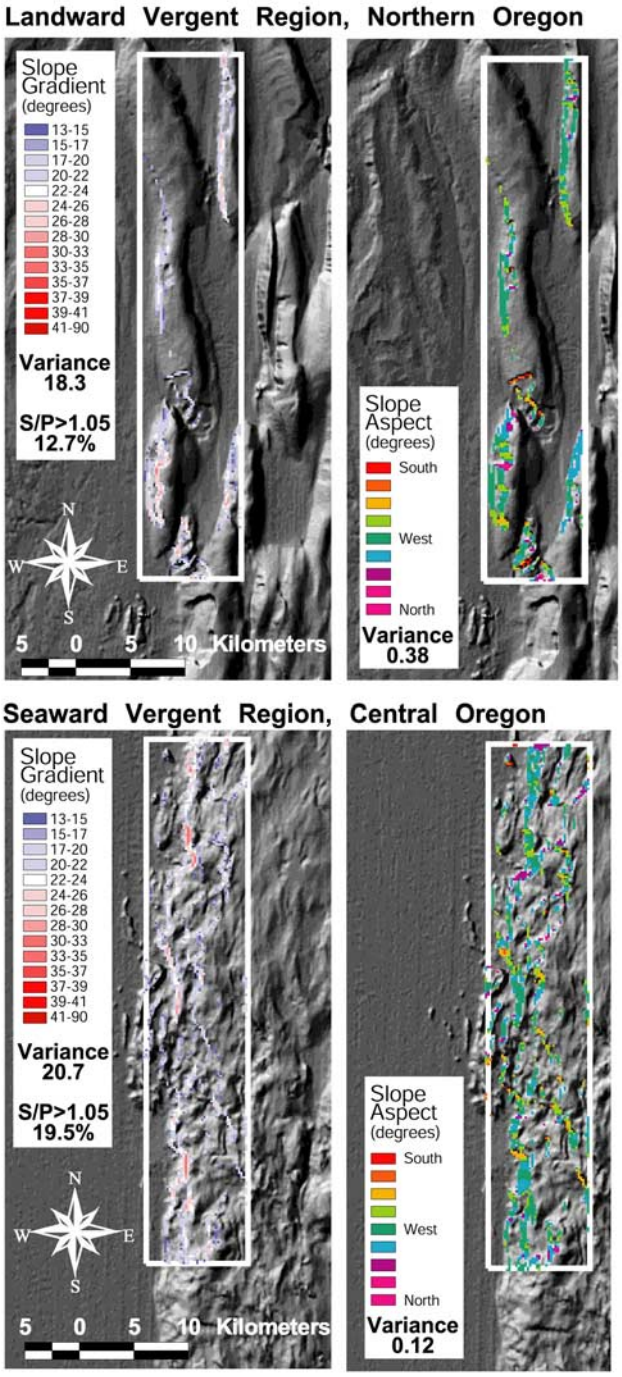

Figure 7. Examples of seafloor roughness from the base of the Oregon continental slope in the landward and seaward vergent regions. Variance of slope gradient and aspect are calculated in a 450 km^2 box at the base of the slope. Only seaward facing slopes are considered to negate the changes in aspect associated with the two sides of an anticlinal ridge. Colors indicate variation of slope gradient and aspect, so the more variation in color, the more the slope is changing shape. Slope gradient and aspect must be considered together as a slope with a diffusional profile may appear very smooth, but have a very high slope variance, and similarly, a smooth and undulating ridge might have a high aspect variance. Slope gradient variance, aspect variance, and percentage of the slope with a surface area to planimetric area ratio (S/P) greater than 1.05 are for the 450 km^2 box only.

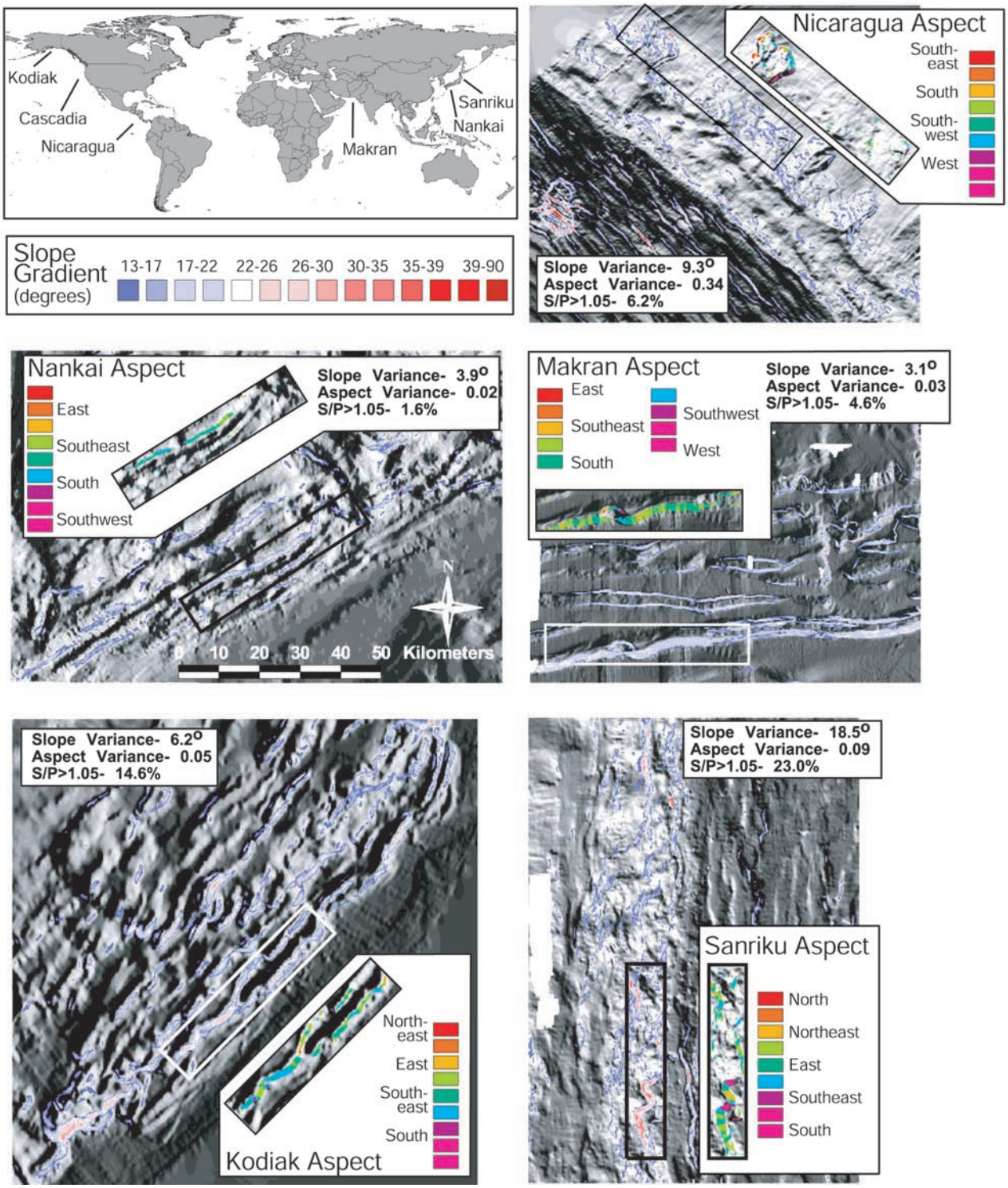

Figure 8. Seafloor roughness by way of slope and aspect variance for the Nicaragua, Nankai, Makran, Kodiak, and Sanriku margins. See Figure 7 for description.

Kodiak slope as evidence by truncation of reflectors at the seafloor, but well defined discrete landslides are absent at the slope base. These accretionary margins have produced historic large magnitude earthquakes [e.g., 1945 Makran, M_w = 7.9; 1964 Alaska, M_w = 9.2), and have apparently had a similar erosive response as Nankai where frequent downslope sediment flows plane off roughness elements.

[39] The Nicaragua, Sanriku and Aleutian (offshore Unimak Island) margins stand in marked contrast to the sedimented, accretionary margins where large-magnitude

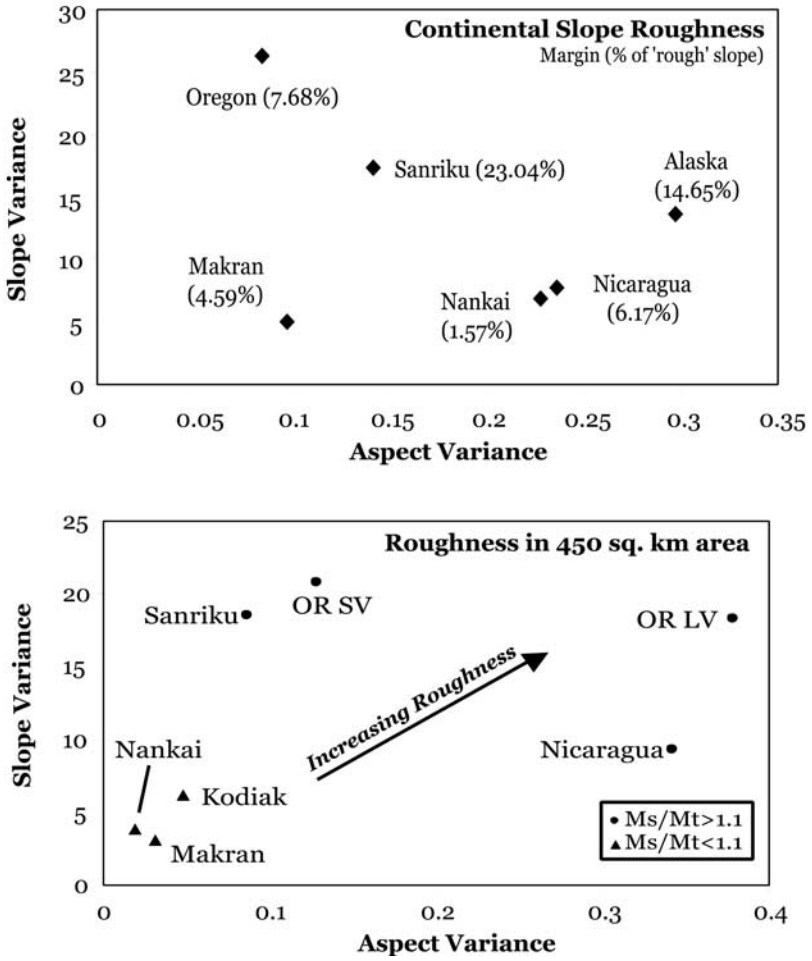

Figure 9. Roughness values (slope gradient and aspect variances) (top) for the entire continental slope and (bottom) for the 450 km^2 region at the base of the slope. Roughness increases away from the origin. Numbers in parentheses represent the percentage of the continental slope's area with a surface area to planimetric area ratio greater than 1.05. In the bottom diagram, circles represent regions where recent earthquakes have produced large tsunami (M_t) compared to the surface wave excitation (M_s), whereas the triangles represent events with tsunamis comparable to the degree of shaking. The italics represent regions without surface wave magnitude (OR SV, Oregon seaward vergent; OR LV, Oregon landward vergent), but fall within the roughness sphere of the margins that produce tsunami earthquakes.

earthquakes occur. Earthquakes tend to have moderate surface wave magnitudes, and produce significant tsunamis. Each of these margins has very large, well-preserved landslide scars (which add roughness) that have not been significantly smoothed by agents of diffusion. Two possible reasons for the existence of these features include (1) the slides are very recent, and not enough time has elapsed since their inception for significant diffusion of the scar to have occurred, (2) the slides represent very old and infrequent (large) events, perhaps associated with less temporally frequent events such as sea level lowstands, rather than recent earthquakes, and rates of bathymetric diffusion are low. Strong shaking associated with earthquakes will likely hasten the diffusion of roughness elements, therefore smooth and highly eroded regions on active convergent margins suggest strong shaking. Rougher margins with well-preserved landslides may have their rough elements preserved because of a lack of sediment available for abrasion. This may be the case in Nicaragua and Sanriku, but Cascadia with its ample sediment supply is an outlier.

[40] There is a temptation to seek a coseismic offshore landsliding source to increase the tsunami magnitude on the margins that have produced tsunami earthquakes, and have candidate landslides preserved in the epicentral regions. However, the 1992 Nicaragua event, captured by modern instrumentation, is interpreted as having a slow source mechanism due to subducting sediment [*Kanamori and Kikuchi*, 1993]. The Sanriku earthquake has also been interpreted as a slow rupture associated with subducted sediments, based on tsunami modeling of tide gauge data [*Tanioka and Satake*, 1996]. There is some debate as to the cause of the 1946 Aleutian's tsunami, as it may have been caused by either a slow source or a coseismic offshore slide [*Johnson and Satake*, 1997; *Fryer and Watts*, 2001], but it is

difficult to reconcile a Pacific basin-wide tsunami with a landslide source offshore Unimak Island alone.

[41] The Cascadia margin offshore Oregon is a combination of two morphologies; it is a sedimented margin with very large and well-preserved landslides. We are able to extrapolate regions of erosion beyond the 2-D seismic lines showing places in the weak and overpressured landward vergent region [*MacKay*, 1995] with continuous smooth, noneroded slopes. The seaward vergent region appears as one might expect on a seismically active margin, but is somewhat different that what is observed in Nankai, Kodiak, and Makran. Rather than smooth slopes with ample erosion on those margins, erosion in the seaward vergent region occurs by way of numerous and overlapping, sometimes discrete, slides throughout the margin [*Goldfinger et al.*, 2000; *McAdoo et al.*, 2000]. As the larger slides (those that are preserved and visible in the multibeam bathymetry data) probably occur less frequently than the smaller slides, these features are probably older, and quite likely predate the last Cascadia event in 1700 A.D. If slides of these magnitudes occurred after each earthquake, there would be very little continental slope remaining after several events.

[42] Slope failure and resultant bathymetry of Nankai, Makran, and Kodiak, and to a somewhat lesser extent on Cascadia's seaward vergent region [*McAdoo et al.*, 2000; *Goldfinger et al.*, 2000], are what one might expect from regions that experience repeated large magnitude subduction zone earthquakes. Evidence from the Cascadia margin points to repeated, margin-wide earthquakes approaching magnitude 9.2, the last as recently as 1700 A.D. [*Atwater et al.*, 1995; *Satake et al.*, 1996; *Goldfinger et al.*, 2003]. If earthquakes are one of the major triggers of erosive events [e.g., *Hampton et al.*, 1996], then we should expect to see a great deal of erosion on this margin. This is especially true if we consider the normally consolidated sediment on the steep flanks of the anticlines [*McAdoo et al.*, 1997].

6. Tsunami Earthquakes in Cascadia

[43] There have been several notable tsunami earthquakes in recent history. The 1896 Sanriku (M_s = 7.2, M_t = 8.6), 1923 Kamchatka (M_s = 7.2, M_t = 8.2), 1946 Aleutians (M_s = 7.4, M_t = 9.3), 1960 Peru (M_s = 6.9, M_t = 7.8), and 1992 Nicaragua (M_s = 7.2, M_t = 7.9 [*Abe*, 1979; *Kanamori and Kikuchi*, 1993]. In each of these events, ground motions were not very severe, yet the amplitude of the associated tsunami excited was unusually high. Furthermore, the slow rupture mechanism in each of these events has been attributed to faulting in shallow subducted sediment [*Kanamori and Kikuchi*, 1993].

[44] It is difficult to reconcile the geomorphology of the Cascadia margin with the strong shaking that would accompany a $M > 9$ earthquake when the morphology of margins with know seismic histories are taken into account. Yet the tsunami deposits in the onshore marshes and turbidites in the offshore sea channels from northern California to Vancouver Island suggest a margin-wide event. Furthermore, the turbidites in the offshore channels suggest shaking strong enough to dislodge large quantities of sediment. Evidence of localized onshore liquefaction in the lower Columbia River also suggests strong shaking during a Cascadia event near the coastline [*Obermeier and Dickenson*, 2000; *Atwater et al.*, 2001].

[45] There are several possible scenarios for past and possibly future Cascadia events that can resolve the apparent discrepancy between the offshore geomorphology and the deposits in the geologic record. The first option, as suggested by *McCaffrey and Goldfinger* [1995], Cascadia may be more likely to produce a series of back-to-back $M\sim8$ events, separated by active strike-slip faults in the forearc, and the tsunami magnitude could be augmented by coseismic landsliding. A second option is a characteristic earthquake (margin-wide or segmented) with a slow source mechanism, perhaps with stronger shaking toward the coast and continental shelf break, and diminishing motion on the continental slope which overlies the weakest part of the plate boundary interface.

[46] *Goldfinger et al.* [2003] suggest that the turbidites in the offshore sea channels are due to strong shaking on the continental margin. They effectively discount several potential mechanisms that could trigger a turbid flow in a canyon including large storm waves, hyperpycnal flows, and teletsunami that load the sediment in a canyon head; however, they do not discount a local tsunami. Their data correlate remarkably well with the on land tsunami deposit records. A local tsunami will have higher amplitudes and frequencies than a tsunami generated by a similar earthquake on the other side of the Pacific Ocean due to the dispersive effects of a propagating wave. Therefore a locally generated tsunami might be able to trigger a canyonhead failure (by way of rapid and high amplitude cyclic loading) and subsequent turbidity current where a teletsunami may not. Another possible explanation for the triggering of turbidity currents in canyon heads would be stronger shaking at the continental shelf break, and diminished shaking on the continental slope where fluid overpressures on the décollement are likely to be higher, which would in turn slow down the rupture propagation.

[47] The distinct difference in geomorphology between the landward and seaward vergent regions leads us to support a hybrid model where the margin is segmented, and the northern landward vergent section produces a slow earthquake and the southern seaward vergent region produces a standard earthquake. In the north, landslides are well preserved, like Nicaragua, Sanriku and offshore Unimak Island, and erosion is limited because the seafloor does not shake very hard. In the south, the margin has a morphology and erosive regime closer to Nankai, Makran and Kodiak, suggesting frequent (relative to sedimentation events) earthquakes that shake hard enough to cause failure in the consolidated sediment, which preserves the scars. That the scars are preserved may suggest shaking not quite as vigorous as that experienced on those margins.

[48] The regional geology supports the supposition that Cascadia might rupture in a slow event. In sites of thick sediment and a well-developed accretionary prism with

weak material as in northern Oregon (due in part to fluid overpressuring [*Moore et al.*, 1995]), the subduction interface may be slipping aseismically [*Byrne et al.*, 1988). This scenario is particularly attractive considering that one of the requisites for landward vergence is a very weak basal décollement caused by elevated fluid pressures due to rapid sedimentation in the region of the Astoria Fan [*MacKay*, 1995]. *Bilek and Lay* [1999] point out that increased fluid pressures in the subduction interface will lower the rigidity of the material, which will in turn reduce the rupture velocity. The geomorphology of the seaward vergent region suggests better coupling, but only two thirds of the incoming section is being frontally accreted in the seaward vergent region [*MacKay et al.*, 1992], which could provide enough material under the slope to slow down the rupture velocity.

[49] The thermal and geodetic modeling of *Hyndman and Wang* [1993] suggests that the updip locked limit of the subduction zone extends to the deformation front, and the downdip limit lies below the continental shelf, between where the 350°C–450°C isotherms meet the subduction interface. The resulting shape of the locked portion of the subduction zone has a very skewed aspect ratio, approximately 90 km by 1000 km, which is exceptional when compared to the shape of other great earthquake rupture zones [*Hyndman and Wang*, 1993]. When the reduction of rigidity (i.e., shear strength) is considered in the overpressured sediments within the subduction interface in the landward vergent region, the aspect ratio (in this region) is further reduced, making it even less similar to other great earthquake rupture areas. Furthermore, *Tanioka and Ruff* [1997] comment on the roughness of the downgoing plate, where large underthrusting earthquakes occur where the subduction interface is smooth (which is the case in Cascadia), and the data of *Bilek and Lay* [1999] suggest that longer duration events occur at shallow depths on the margins with smooth plate interfaces. Deeper, shorter duration events are precluded by the thick, insulating sediment covering young, warm Juan de Fuca crust which limits the downdip extent of Cascadia subduction zone [*Hyndman and Wang*, 1993]. It is possible that slip begins at some portion of the narrow locked zone, propagates up dip, then slows based on the rigidity and/or fluid pressure of the subduction interface [*Pelayo and Wiens*, 1992; *Polet and Kanamori*, 2000], which is likely to be slower in regions of high sedimentation rates. During this updip propagation, splay faults in the accretionary prism may distribute the slip [*Fukao*, 1979] causing any one region to be moved less and slower, therefore reducing the likelihood of slope failure.

7. Conclusions

[50] On the basis of the geomorphologic and subsurface erosive regimes of several convergent margins, we suggest that the central portion of the Cascadia subduction zone produces so-called tsunami earthquakes, where the magnitude of the tsunami is much larger than the surface wave magnitude (or degree of shaking) would suggest. The Nankai margin, offshore SW Japan, very similar to Cascadia in tectonic regime and geologic structure, is substantially smoothed by downslope erosive sediment flows most likely triggered by the great earthquakes ($M_s > 8$) that occur every 100–300 years. The Makran (Pakistan) and Kodiak (Alaska) margins exhibit similar erosive morphologies and have had historic, large surface wave magnitude earthquakes. Margins that have produced historical tsunami earthquakes tend to have well-preserved landslides that add roughness elements to the slope. Quantitative analysis of the lower slope seafloor roughness shows that margins that produce tsunami earthquakes are substantially rougher. This is likely because the margins that produce slow earthquakes have the subduction zone interface weakened by the subducted sediment. The continental margin is therefore lacking in the sediment that would act to smooth the slope. The large landslides are most likely very old features, possibly associated with the last sea level lowstand, and have been preserved by the lack of downslope erosive flows. The frequencies of seismic energy generated by the slow source mechanism are sufficient to generate a tsunami, but probably too low to generate accelerations that would cause slope failures.

[51] The northern Oregon section of the Cascadia margin has many of the landmarks of a slow earthquake-producing margin. Elevated fluid pressures in the northern Oregon accretionary prism, and nonaccreted sediment in the seaward vergent region reduce the updip extent of the seismogenic zone, and high temperatures due to young crust and insulating sediment reduce the downdip limit of the seismogenic zone. Elevated fluid pressures in the décollement will also have the effect of reducing rigidity, further dropping the rupture velocity. The geomorphology of the accretionary wedge offshore Oregon, with very steep slopes with limited erosion, well preserved landslides, and landward verging structures support the conclusion that when the Cascadia megathrust event happens, the seafloor does not shake hard enough to fail even the most delicate of landforms. The best model for a Cascadia event is a slow earthquake, or perhaps a series of slow earthquakes, that produces a significant margin-wide tsunami, perhaps with zones of strong shaking (in southern Oregon) where interplate coupling is stronger.

[52] **Acknowledgments.** This study was funded by a Research Opportunity Award to B. G. M. through a National Science Foundation grant to J. C. Moore (OCE-9802264), University of California, Santa Cruz. Additional support for M. K. C. and J. M. came from the Vassar College Environmental Research Fund. We thank N. Bangs, S. Gulick, and T. Shipley of the University of Texas Institute of Geophysics and G. Moore of the University of Hawaii for collection and processing of the 3-D seismic data off SW Japan. Landmark Graphics Corporation provided seismic processing and interpretation software used for this research at UC Santa Cruz. Seismic Microtechnologies provided the seismic interpretation software to Vassar as part of their Educational Grants Program. Multibeam bathymetry was kindly supplied by C. Ranero (GEOMAR) and K. Satake (Advanced Industrial Science and Technology, Japan). The manuscript was substantially improved by the comments of B. Wernicke, K. Whipple, B. Atwater, C. Goldfinger, and D. Walker.

References

Abe, K. (1979), Size of great earthquakes of 1837–1974 inferred from tsunami data, *J. Geophys. Res.*, *84*, 1561–1568.

Abe, K. (1994), Instrumental magnitudes of historical earthquakes, 1892–1898, *Bull. Seismol. Soc. Am.*, *84*, 415–425.

Ando, M. (1975), Source mechanisms and tectonic significance of historical earthquakes along the Nankai Trough, *Japan, Tectonophysics*, *27*, 119–140.

Atwater, B. F., et al. (1995), Summary of coastal geologic evidence for past great earthquakes at the Cascadia subduction zone, *Earthquake Spectra*, *11*, 1–18.

Atwater, B. F., et al. (2001), Grouted sediment slices show signs of earthquake shaking, *Eos Trans. AGU*, *82*, 603, 608.

Bilek, S. L., and T. Lay (1999), Comparison of depth dependent fault zone properties in the Japan Trench and Middle America Trench, *Pure Appl. Geophys.*, *154*, 433–456.

Byrne, D. E., D. M. Davis, and L. R. Sykes (1988), Loci and maximum size of thrust earthquakes and the mechanisms of the shallow region of subduction zones, *Tectonics*, *7*, 833–857.

Byrne, D. E., L. R. Sykes, and D. M. Davis (1992), Great thrust earthquakes and aseismic slip along the plate boundary of the Makran subduction zone, *J. Geophys. Res.*, *97*, 449–478.

Cadet, J. P., et al. (1987), Deep scientific dives in the Japan and Kuril trenches, *Earth Planet. Sci. Lett.*, *83*, 313–328.

Cochrane, G. R., J. C. Moore, M. E. MacKay, and G. F. Moore (1994), Velocity-porosity model of the Oregon accretionary prism from seismic reflection and refraction data, *J. Geophys. Res.*, *99*, 7033–7043.

DeMets, C., R. G. Gordon, D. F. Argus, and S. Stein (1990), Current plate motions, *Geophys. J. Int.*, *101*, 425–478.

Fisher, M. A., E. R. Flueh, D. W. Sholl, T. Parsons, R. E. Wells, A. Trehu, U. ten Brink, and C. S. Weaver (1999), Geologic processes of accretion in the Cascadia subduction zone west of Washington State, *Geodynamics*, *27*, 277–288.

Fruehn, J., R. von Huene, and M. A. Fisher (1999), Accretion in the wake of terrane collision: The Neogene accretionary wedge off Kenai Peninsula, Alaska, *Tectonics*, *18*, 263–277.

Fryer, G. J., and P. Watts (2001), Motion of the Ugamak Slide, probable source of the tsunami of 1 April 1946, in *Proceedings of the International Tsunami Symposium 2001*, pp. 683–694, NOAA Pac. Mar. Environ. Lab., Seattle, Wash.

Fryer, G. J., P. Watts, and L. F. Pratson (2004), Source of the great tsunami of 1 April 1946: A landslide in the upper Aleutian forearc, *Mar. Geol.*, *203*, 201–208.

Fukao, Y. (1979), Tsunami earthquakes and subduction processes near deep-sea trenches, *J. Geophys. Res.*, *84*, 2303–2314.

Goldfinger, C., L. D. Kulm, L. C. McNeill, and P. Watts (2000), Superscale failure of the southern Oregon Cascadia margin, *Pure Appl. Geophys.*, *157*, 1189–1226.

Goldfinger, C., C. H. Nelson, and J. E. Johnson (2003), Holocene earthquake records from the Cascadia subduction zone and northern San Andreas Fault based on precise dating of offshore turbidites, *Annu. Rev. Earth Planet. Sci.*, *31*, 555–577.

Grim, P. (1992), Dissemination of NOAA/EEZ multibeam bathymetric data, NOS, in *1991 Exclusive Economic Zone Symposium: Working Together in the Pacific EEZ Proceedings*, edited by M. Lockwood and B. A. McGregor, *U.S. Geol. Surv. Circ.*, *1092*, 102–109.

Hampton, M. A., H. J. Lee, and J. Locat (1996), Submarine landslides, *Rev. Geophys.*, *34*, 33–59.

Hyndman, R. D., and K. Wang (1993), Thermal constraints on the zone of major thrust earthquake failure: The Cascadia subduction zone, *J. Geophys. Res.*, *98*, 2039–2060.

Johnson, J. M., and K. Satake (1997), Estimation of seismic moment and slip distribution of the April 1, 1946 Aleutian tsunami earthquake, *J. Geophys. Res.*, *102*, 11,765–11,774.

Kanamori, H., and M. Kikuchi (1993), The 1992 Nicaragua earthquake: A slow tsunami earthquake associated with subducted sediments, *Nature*, *361*, 714–716.

Karig, D. E. (1986), Physical properties and mechanical state of accreted sediments in the Nankai Trough, SW Japan, in *Structural Fabrics in Deep Sea Drilling Project Cores from Forearcs*, edited by J. C. Moore, *Mem. Geol. Soc. Am.*, *166*, 117–133.

Karl, H. A., and R. Carlson (1996), Alaskan EEZ, in *Geology of the United States' Seafloor: The View from GLORIA*, edited by J. Gardner, M. E. Field, and D. C. Twichell, pp. 251–254, Cambridge Univ. Press, New York.

Kayen, R. E., and H. Lee (1993), Slope stability in regions of seafloor gas hydrate, Beaufort Sea continental slope, in *Submarine Landslides: Selected Studies in the U.S. Exclusive Economic Zone*, edited by W. C. Schwab, H. Lee, and D. C. Twichell, *U.S. Geol. Surv. Bull.*, *2002*, 97–103.

Kopp, C., J. Fruehn, E. R. Flueh, C. Reichert, N. Kukowski, J. Bialas, and D. Klaeschen (2000), Structure of the Makran subduction zone from wide angle and reflection seismic data, *Tectonophysics*, *329*, 171–191.

Kukowski, N., T. Schillihorn, K. Huhn, U. von Rad, S. Husen, and E. R. Flueh (2001), Morphotectonics and mechanics of the central Makran accretionary wedge off Pakistan, *Mar. Geol.*, *173*, 1–19.

Kulm, L. D., et al. (1986), Oregon subduction zone: Venting, fauna, and carbonates, *Science*, *231*, 561–566.

Li, C., and A. L. Clark (1991), SeaMARCII study of a giant submarine slump on the northern Chile continental slope, *Mar. Geotechnol*, *10*, 257–268.

MacKay, M. E. (1995), Structural variation and landward vergence at the toe of the Oregon accretionary prism, *Tectonics*, *14*, 1309–1320.

MacKay, M. E., G. F. Moore, G. R. Cochrane, J. C. Moore, and L. D. Kulm (1992), Landward vergence and oblique structural trends in the Oregon margin accretionary prism: Implications and effect on fluid flow, *Earth Planet. Sci. Lett.*, *109*, 477–491.

McAdoo, B. G., D. L. Orange, E. Screaton, H. Lee, and R. Kayen (1997), Slope basins, headless canyons, and submarine palaeoseismology of the Cascadia accretionary complex, *Basin Res.*, *9*, 313–324.

McAdoo, B. G., L. F. Pratson, and D. L. Orange (2000), Submarine landslide geomorphology, US continental slope, *Mar. Geol.*, *169*, 103–136.

McCaffrey, R., and C. Goldfinger (1995), Forearc deformation and great subduction earthquakes: Implications for Cascadia offshore earthquake potential, *Science*, *267*, 856–859.

Moore, G. F., et al. (2001), Data report: Structural setting of the Leg 190 Muroto transect, *Proc. Ocean Drill. Program Initial Rep., 190* [CD-ROM].

Moore, J. C., G. F. Moore, G. R. Cochrane, and H. J. Tobin (1995), Negative-polarity reflections along faults of the Oregon accretionary prism; indicators of overpressuring, *J. Geophys. Res.*, *100*, 12,895–12,906.

Obermeier, S. F., and S. E. Dickenson (2000), Liquefaction evidence for the strength of ground motions resulting from late Holocene Cascadia subduction earthquakes with emphasis on the event of 1700 AS, *Bull. Seismol. Soc. Am.*, *90*, 876–896.

O'Leary, D. W. (1993), Submarine mass movement, a formative process of passive continental margins: The Munson-Nygren landslide complex and the Southeast New England landslide complex, in *Submarine Landslides: Selected Studies in the U.S. Exclusive Economic Zone*, edited by W. C. Schwab, H. Lee, and D. C. Twichell, *U.S. Geol. Surv. Bull.*, *2002*, 97–103.

Pelayo, A. M., and D. A. Wiens (1992), Tsunami earthquakes: Slow thrust-faulting events in the accretionary wedge, *J. Geophys. Res.*, *97*, 15,321–15,337.

Polet, J., and H. Kanamori (2000), Shallow subduction zone earthquakes and their tsunamigenic potential, *Geophys. J. Int.*, *142*, 684–702.

Ranero, C. R., R. von Huene, E. Flueh, M. Duarte, D. Baca, and K. McIntosh (2000), A cross section of the convergent Pacific margin of Nicaragua, *Tectonics*, *19*, 335–357.

Satake, K. (1994), Mechanism of the 1992 Nicaragua tsunami earthquake, *Geophys. Res. Lett.*, *21*, 2519–2522.

Satake, K., K. Shimazaki, Y. Tsuji, and K. Ueda (1996), Time and size of a giant earthquake in Cascadia inferred from Japanese tsunami records of January 1700, *Nature*, *379*, 246–249.

Seno, T., S. Stein, and A. E. Gripp (1993), A model for the motion of the Philippine Sea plate consistent with NUVEL-1 and geological data, *J. Geophys. Res.*, *98*, 17,941–17,948.

Tanioka, Y., and L. J. Ruff (1997), Source time functions, *Seismol. Res. Lett.*, *68*(3), 386–400.

Tanioka, Y., and K. Satake (1996), Fault parameters of the 1896 Sanriku tsunami earthquake estimated from tsunami numerical modeling, *Geophys. Res. Lett.*, *23*, 1549–1552.

von Huene, R., and R. Culotta (1989), Tectonic erosion at the front of the Japan trench convergent margin, *Tectonophysics*, *160*, 75–90.

von Huene, R., D. Klaeschen, B. Cropp, and J. Miller (1994), Tectonic structure across the accretionary and erosional parts of the Japan Trench margin, *J. Geophys. Res.*, *99*, 22,349–22,361.

von Rad, U., and H. Doose (Eds.) (1998), MAKRAN II, the Makran accretionary wedge off Pakistan: Tectonic evolution and fluid migration, RV *Sonne* cruise SO 130, report, Bundesanst. für Geowiss. und Rohstoffe BGR, Hannover, Germany.

Wang, K. (2000), Stress-strain paradox, plate coupling, and forearc seismicity at the Cascadia and Nankai subduction zones, *Tectonophysics*, *319*, 321.

Yamazaki, T., and Y. Okamura (1989), Subducting seamounts and deformation of overriding forearc wedges around Japan, *Tectonophysics*, *160*, 207–229.

M. K. Capone, B. G. McAdoo, and J. Minder, Department of Geology, Vassar College, P.O. Box 735, Poughkeepsie, NY 12604, USA. (brmcadoo@vassar.edu)